Polarized polariton condensates and coupled *XY* models

Jonathan Keeling*
Cavendish Laboratory, University of Cambridge, J. J. Thomson Avenue, Cambridge CB3 0HE, United Kingdom
(Received 14 April 2008; revised manuscript received 25 October 2008; published 17 November 2008)

Microcavity polaritons, which at low temperatures can condense to a macroscopic coherent state, possess a polarization degree of freedom. This paper discusses the phase diagram of such a system, showing the boundaries between differently polarized condensates. The Bogoliubov approximation is shown to have problems in describing the transition between differently polarized phases; the Hartree-Fock-Popov approximation performs better, and compares well to exact results that can be used in the limit where the left- and right-circular polarization states decouple. The effects on the phase boundary of various symmetry breaking terms present in real microcavities are also considered.

DOI: 10.1103/PhysRevB.78.205316 PACS number(s): 71.36.+c, 03.75.Mn

I. INTRODUCTION

The recent experimental progress in attaining spontaneous coherence in a thermalized degenerate gas of microcavity polaritons[1–7] has extended the range of systems in which quantum condensation may be studied. As well as sharing many features with previous examples of quantum condensates (such as superfluid helium, cold atoms and superconductors) polariton condensates possess naturally a number of distinguishing features (see, e.g., Refs. 8 and 9 and references therein).

This paper considers the combined effect of two such features of condensed polaritons: their polarization degree of freedom and confinement to two dimensions. Recent works[10–12] have considered some effects arising from the polarization degree of freedom; including a tentative phase diagram[11] derived from a zero-temperature mean-field theory, this phase diagram implied a transition temperature which vanished at a critical magnetic field. This paper has two aims: first to examine more carefully the phase diagram (critical temperature vs magnetic field) of a polarized polariton condensate, this is found to be rather different to that in Ref. 11; second to discuss how the phase diagram would be affected by terms breaking polarization rotation symmetry that are expected in real microcavities.

In order to discuss the effects of polarization on the polariton phase diagram in the most transparent way, this paper makes various simplifications: it considers an infinite two-dimensional polariton system, in thermal equilibrium. In addition, the model described in Refs. 11 and 12 is used, which is applicable in the limit of very low densities and temperatures, where only the low energy part of the lower polariton dispersion—with a quadratic dispersion—is thermally populated. At higher densities, one must take account of the nonquadratic dispersion of lower polaritons, and the possibility of other excitations depleting the condensate.[4] These considerations will change the dependence of critical temperature on density, but the nature of the possible polarized phases and topology of the phase diagram as a function of magnetic field should not significantly change.

Current experiments remain some distance from this limit of low temperature, low density, infinite, clean, equilibrium systems. The experimental densities are at the point where other excitations start to become relevant,[4] the polariton clouds are relatively small and their profiles strongly affected by photonic disorder[3,5,6] or trapping potentials,[2] and pumping and decay have noticeable effects.[4–6] It does however remain a useful exercise to understand how spin degrees of freedom modify the phase diagram in the ideal system first, before including these various extra complications, both to understand the nature of the possible phases and transitions and also to have a basis from which one can investigate the differences introduced by pumping, decay, disorder and finite sizes. In addition, improvements in fabrication of microcavity samples can be expected to reduce the effect of disorder, and increase the lifetime of polaritons, opening the possibility that future generations of experiments might come closer to the idealized model discussed here. A review of how some of these effects of disorder, pumping, decay, etc. affect coherence in current microcavity polariton experiments can be found for example in Ref. 9.

II. MODEL

The polarization of the polariton can be written as a two-component complex spinor $\vec{\psi}$,

$$\vec{\psi}=\begin{pmatrix}\psi_x\\ \psi_y\end{pmatrix}=\frac{l}{\sqrt{2}}\begin{pmatrix}1\\ i\end{pmatrix}+\frac{r}{\sqrt{2}}\begin{pmatrix}1\\ -i\end{pmatrix}. \tag{1}$$

Here l and r are complex coefficients, describing the state in the basis of left- and right-circular polarizations. The model of Ref. 11 in this basis is

$$H-\mu N=\frac{\hbar^2|\nabla l|^2}{2m}+\frac{\hbar^2|\nabla r|^2}{2m}-(\mu+\Omega)|l|^2-(\mu-\Omega)|r|^2+\frac{1}{2}[U_0(|l|^4+|r|^4)+(U_0-2U_1)2|l|^2|r|^2]. \tag{2}$$

The term Ω describes a magnetic field that favors either left- or right-circular polarization. From this point onwards, $\hbar=1$. In 2D the form of the phase diagram is controlled by two dimensionless parameters, mU_0 and $(U_0-2U_1)/U_0$. For mU_0, estimates including effects of excitonic disorder[4] give $U_0\simeq 3\ \mu\mathrm{eV}(\mu\mathrm{m})^2$, and the polariton mass $1/m=7600\ \mu\mathrm{eV}(\mu\mathrm{m})^2$ leads to $mU_0\simeq 4\times 10^{-4}$. Due to the ten-

dency toward biexciton formation, opposite polarizations of polaritons attract, hence $0 > U_0 - 2U_1 > -U_0$; at $\Omega = 0$ this implies $|l| = |r|$ describing linear polarization of light.[11] For the typical values relevant for microcavity polaritons $|U_0 - 2U_1| \ll U_0$; i.e., the interaction between left- and right-circularly polarized light is relatively small;[13] a typical estimate is $(U_0 - 2U_1) = -0.1U_0$. The model of Eq. (2) has been studied in the context of atomic condensation, e.g., Ref. 14, where topological defects and phase separation were investigated; as discussed there, phase separation requires $U_1 < 0$, so it is not considered here.

III. CALCULATING CRITICAL TEMPERATURE

In an infinite two-dimensional system, for a single component Bose gas, it is well known that the phase transition is a Berezhinskii-Kosterlitz-Thouless (BKT) transition. Above the BKT transition vortices proliferate, leading to exponentially decaying correlations; below there is a nonzero superfluid density, and a quasicondensate density, but at long distances phase fluctuations lead to power-law decay of correlations. To see how this is modified in a spinor Bose gas, one needs to consider the elementary vortices of the model in Eq. (2). As discussed by Ref. 12, these elementary vortices are separate vortices of left- and right-circularly polarized light. Thus, to a first approximation, the critical temperature occurs when the phase stiffness of l or r becomes small enough that vortices of l or r will proliferate. Note, however, that although the elementary vortices are separate vortices of l and r, as long as $U_0 - 2U_1 \neq 0$ then the long wavelength phase fluctuations are mixtures[10,11] of l and r.

When l and r vortices are independent, the critical temperature at which vortices proliferate is given by $\rho_s^{l,r} = (2/\pi) m k_B T$ where $\rho_s^{l,r}$ are the phase stiffness of each species. Section IV will show that in the absence of symmetry breaking terms beyond the model in Eq. (2), it is appropriate to treat these transitions independently, and will discuss how symmetry breaking terms modify this argument. This paper will present the phase diagram of critical temperature as a function of magnetic field, working at a fixed total density of polaritons. With such an approach, to calculate the phase boundary one will require expressions for the total density $\rho_{\text{total}}(\mu, \Omega, T)$ of the coupled system and for the superfluid densities for each separate polarization $\rho_s^{l,r}$; the following sections will discuss calculating these quantities.

A. Decoupled case, $U_0 = 2U_1$

The interaction between left and right polarizations is relatively weak, and so it is worth first considering the special case $U_0 = 2U_1$ for which the polarizations decouple. This case is simple for two reasons. First, it is clear that there are two completely independent phase transitions associated with BKT transitions for the l and r polarizations. Second, one may reuse the equation of state $\rho_1(\mu, T)$ and critical chemical potential μ_{c1} for a one-component 2D Bose gas, which allows a comparison between the exact equation of state and various perturbative approximations.

The equation of state for a single-component Bose gas, calculated using a Monte Carlo (MC) method, is described in Ref. 15. In terms of the single-component equation of state, the density for the two-component model may be written as $\rho_{\text{total}}(\mu, \Omega, T) = \rho_1(\mu - \Omega, T) + \rho_1(\mu + \Omega, T)$, and so the critical temperatures at field Ω are the solutions of the equation

$$\rho_{\text{total}} = \rho_1(\mu_{c1}, T_c) + \rho_1(\mu_{c1} \pm 2\Omega, T_c). \quad (3)$$

In two dimensions, the equation of state can be written as $\rho_1(\mu, T) = T\tilde{\rho}_1(\mu/T)$ and the critical chemical potential scales as $\mu_{c1} = x_c T$. Given $\tilde{\rho}_1(x)$ (as shown in Fig. 1) and x_c, it is straightforward to find $T_c(\Omega)$ for the two-component case. The two-component equation, Eq. (3), becomes

$$\rho_{\text{total}} = T_c[\tilde{\rho}_1(x_c) + \tilde{\rho}_1(x_c \pm 2\Omega/T_c)] \equiv T_c F(\Omega/T_c). \quad (4)$$

The phase boundary calculated from this equation of state is shown by the solid line in Fig. 2. The solution as $T_c \to 0$ requires $\tilde{\rho}_1 \to \infty$, which for the MC calculation occurs at a finite and nonzero Ω as $\Omega/T_c \to \infty$.

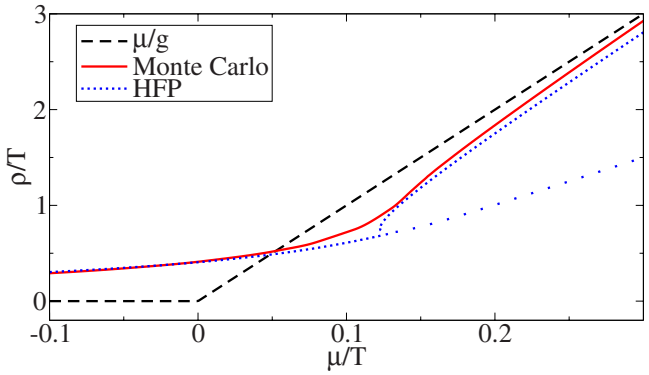

FIG. 1. (Color online) Equation of state, $\rho(\mu, T) = Tf(\mu, T)$ for a 2D single-component Bose gas, as given by HFP approximation and Monte Carlo results of Ref. 15. The wider spaced dots for the lower branch of the HFP calculation are unphysical; they lead to the corresponding wider spaced dots in Fig. 2.

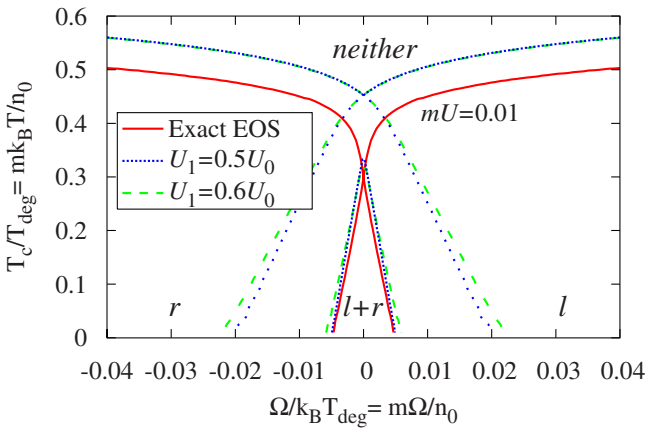

FIG. 2. (Color online) Critical temperature vs magnetic field (both measured in units of $k_B T_{\text{deg}} = n_0/m$), at fixed total density. Labels l, r, $l+r$ and *neither* state which polarizations are superfluid. Red solid line: Monte Carlo results valid when $U_1 = 0.5U_0$. Blue dotted: HFP results for the same parameters. Green dashed: HFP for a weak interpolarization interaction. The HFP lines at intermediate temperatures, with wider spaced dots and dashes, are unphysical.

Physically, the phases marked l and r correspond to pure circular polarizations, while the phase $l+r$ will have an elliptical polarization in general, and at $\Omega=0$, where the densities of l and r match, it will be linear. Reference 11 showed that at $T=0$, at the critical Ω separating l from $l+r$, there is a quadratic gapless mode corresponding to fluctuations of r. It was suggested there that this mode prevents superfluidity, and so suppresses the transition temperature to zero at this point. However, this mode corresponds to excitations of r which have decoupled from those of l at this point, and so a force acting only on l can still have a superfluid response; this is obviously the case when $U_0=2U_1$, but remains true even for nonzero interactions.

B. General case, $U_0 \neq 2U_1$

For $U_0 \neq 2U_1$, one would either need to perform new numerical simulations or find an appropriate perturbation scheme. The simplest scheme one might consider is the Bogoliubov approach, which considers only the self-energy due to interactions with the condensate. This approach is however incapable of describing transitions such as that between $l+r$ both condensed and just l condensed. In the phase with just l condensed, as $\mu \to \Omega$, the density of r will diverge, and so the density of l (and hence the critical temperature) will go to zero. Considering this Bogoliubov approximation as applied to the case of $U_0=2U_1$, this zero of the critical temperature can be understood as follows. If one plots the Bogoliubov approximation to the equation of state $\tilde{\rho}_1(x)$, there is an unphysical divergence as $x=\mu/T \to 0^-$, while the exact equation of state is smooth. It is clear that an unphysical divergence of $\tilde{\rho}_1(x)$ at a finite value of x leads to an unphysical extra solution of Eq. (4) at $\Omega=0$, $T=0$. This would produce a phase diagram like that of Ref. 11, but is an artifact of neglecting the self-energy due to the noncondensed particles.

A better approach is the Hartree-Fock-Popov (HFP) method, see, e.g., Refs. 16 and 17, which includes self-energies due to the population of thermal and quantum fluctuations, but neglects anomalous correlations $\langle l^\dagger l^\dagger \rangle$, etc. By including self-energies due to fluctuation populations, there is no divergence of density, as a large density ρ^r would lead to a large self-energy, reducing the effective chemical potential for r.

The HFP method divides each polarization into a quasicondensate density, $\rho_0^{l,r}$ and fluctuation density $\rho_f^{l,r}$. Both densities contribute to the gap equation:

$$U_0(\rho_0^l + 2\rho_f^l) + (U_0 - 2U_1)(\rho_0^r + \rho_f^r) = \mu + \Omega, \tag{5}$$

$$U_0(\rho_0^r + 2\rho_f^r) + (U_0 - 2U_1)(\rho_0^l + \rho_f^l) = \mu - \Omega. \tag{6}$$

As in Ref. 17, the fluctuation density is found from the correlation function $\langle l^\dagger(\mathbf{x}) l(0) \rangle = \tilde{\rho}^l(\mathbf{x}) \exp[-\Lambda^l(\mathbf{x})]$. The exponent $\Lambda^l(\mathbf{x})$ describes the power-law decay of correlations at long distances, and the prefactor $\tilde{\rho}^l(\mathbf{x})$ describes decay from $\rho_0^l + \rho_f^l$ at $\mathbf{x}=0$ to the quasicondensate density ρ_0^l at intermediate distances. Thus $\rho_f^l = \tilde{\rho}^l(0) - \tilde{\rho}^l(\infty)$. The correlation function is found from the effective action for density and phase fluctuations. Writing $l = \sqrt{\rho_0^l + \pi^l} e^{i\theta^l}$ (and similarly for r), one may define $\delta\Psi^\dagger = (\theta^l, \pi^l, \theta^r, \pi^r)$, in terms of which

$$\delta S = \sum_{\omega,k} \delta\Psi^\dagger(\omega,k) \mathcal{G}^{-1}(\omega,k) \delta\Psi(\omega,k),$$

$$\mathcal{G}^{-1} = \begin{pmatrix} 2\rho_0^l \epsilon_k & -\omega & 0 & 0 \\ \omega & U_0 + \dfrac{\epsilon_k}{2\rho_0^l} & 0 & (U_0 - 2U_1) \\ 0 & 0 & 2\rho_0^r \epsilon_k & -\omega \\ 0 & (U_0 - 2U_1) & \omega & U_0 + \dfrac{\epsilon_k}{2\rho_0^r} \end{pmatrix}. \tag{7}$$

Because of the spinor structure, the current-current response functions (and hence the superfluid density) have a tensor structure. For example, left superfluid density is given by $\rho_s^l = (\rho_0^l + \rho_f^l) - \rho_n^l$ where $\rho_n^l = m\chi_T^{ll}$ is the normal density, found from the transverse part of the current-current response function,

$$\chi_{ij}^{\alpha\beta} = \sum_{\omega,k} \mathrm{Tr}[\mathcal{G}(k,\omega) \gamma_i^\alpha(k,k) \mathcal{G}(k,\omega) \gamma_j^\beta(k,k)], \tag{8}$$

and γ_i^α, the current vertex is (for $\alpha=l$)

$$\gamma_i^l(k,k) = \frac{k_i}{m} \begin{pmatrix} \sigma_2 & 0 \\ 0 & 0 \end{pmatrix}, \quad \sigma_2 = \begin{pmatrix} 0 & -i \\ i & 0 \end{pmatrix}. \tag{9}$$

The above method gives the total density and superfluid densities when both polarizations are condensed, and so gives the lower temperature boundaries shown in Fig. 2. The HFP method can also be adapted to find the higher temperature boundary between a single polarization condensate and the normal state. Consider the case when only l is condensed; in this case the total density is $\rho_{\mathrm{total}} = \rho_0^l + \rho_f^l + \rho_f^r$, and the gap equation is just Eq. (5) with $\rho_0^r = 0$. With a single condensate in the HFP approximation, there is no coupling between the fluctuations of the l and r polarizations, but only mean-field shifts from the quasicondensate density, hence, the inverse Green's function for fluctuations of l is given by the top left 2×2 block of Eq. (7). For fluctuations of r, one has $\rho_f^r = \Sigma_k n_B(\epsilon_k + \tilde{\Sigma})$, where $\tilde{\Sigma}$ incorporates both self-energy and chemical potential, and is given by

$$\tilde{\Sigma} = 2U_0\rho_f^r + (U_0 - 2U_1)(\rho_0^l + \rho_f^l) - (\mu - \Omega).$$

Eliminating μ using the gap equation, Eq. (5), this becomes

$$\tilde{\Sigma} = (U_0 + 2U_1)\rho_f^r - 2U_1\rho_0^l - (U_0 + 2U_1)\rho_f^l + 2\ \Omega.$$

Figure 2 clearly shows that the HFP approximation cannot accurately describe the entire phase boundary, even when $U_0=2U_1$. Although the low temperature boundary calculated by the HFP and exact equation of state match well, the high temperature boundaries match less well, and worse yet the critical temperatures do not join at $\Omega=0$. This failure is because the HFP equation of state is discontinuous at the transition, and so is inaccurate when the high temperature transition is close to the critical region of the low temperature boundary. However, far from the critical region the HFP approximation is reasonable, i.e., at least as good as the HFP approximation would be for a single-component gas.

Despite its failings, the HFP method is valuable. First it shows that the effect of weak interpolarization interactions on the critical temperature is small. Second it reveals an intriguing property of the transverse current-current response function at zero temperature. In a single-component condensate this vanishes, meaning the entire system is superfluid. For coupled polarizations it does not vanish, but instead one has $\chi_T^{ll}=\chi_T^{rr}=-\chi_T^{lr}=-\chi_T^{rl}\neq 0$. This identity ensures that a force acting on the total density has a longitudinal (i.e., superfluid) response, but a force acting on only one polarization need not. This is expected, since there is overall Galilean invariance for a change of velocity of both polarizations, but not under changes of the velocity of just one polarization. This zero-temperature transverse response is however small, $m\chi_T^{ll}/\rho_{\text{total}}\propto mU_0$, as it arises due to the quantum condensate depletion.

IV. SYMMETRY BREAKING EFFECTS IN NONIDEAL CAVITIES

The discussion so far is based on separate BKT transitions associated with the proliferation of each kind of vortex; i.e., the effective action is that of an XY model:

$$\frac{S}{k_BT}=-\sum_{\langle ij\rangle}[K^l\cos(\theta_i^l-\theta_j^l)+K^r\cos(\theta_i^r-\theta_j^r)]. \quad (10)$$

where $K^{l,r}=\rho_s^{l,r}/(mk_BT)$. This section discusses some possible corrections to this effective action that may change the critical behavior. Three effects that are considered in detail below are as follows. The first is short-range attraction between vortices of θ^l and θ^r due to density-density interactions, which are already present in the model of Eq. (2). The other two effects concern reductions in symmetry present in real cavities. Even in an ideal quantum well, the symmetry group for zinc-blende structures is not cylindrical, but D_{2d} (Ref. 18); this means there is a preferred pair of axes, and so interactions between polarizations of light do not have complete rotation symmetry.[11] When there is asymmetry between the quantum well interfaces, this symmetry is yet further reduced to C_{2v},[19,20] leading to a preferred linear polarization, causing a splitting of the quadratic polarization terms. Such a splitting can be induced by applying an electric field along the growth direction;[21] even without an applied field, such a reduction of symmetry is observed in current experiments.[1,3] These two types of symmetry reduction lead to perturbations that prefer certain phase relationships between the l and r fields, and so modify the order parameter space, hence change the behavior of the phase transitions. Another type of symmetry reduction concerns splitting between transverse electric (TE) and transverse magnetic (TM) modes due both to the cavity and exciton-photon coupling;[8,22,23] this leads to an interesting coupling between gradients of l and r fields,[24] which may shift the transition but does not change the symmetry of the order parameter space so it is not considered in detail here. Section IV A describes how the above considerations should be incorporated as perturbations to Eq. (10), and Sec. IV B then discusses their effect on the phase boundary.

A. Nature of perturbations to Eq. (10)

The short-range attraction between opposite vortices arises because when $U_0\neq 2U_1$, a vortex of one polarization is associated with a density modulation of the other (see Ref. 12). Thus a configuration with a vortex in each polarization has a lower energy when these vortices are colocated, independent of whether the phase windings of each polarization are aligned or antialigned. This energy difference ΔE is finite, and numerical analysis for $\Omega=0$ and small $(2U_1-U_0)/U_0$ gives $\Delta E/E_c\propto(2U_1-U_0)/U_0$, where E_c is the core energy of a single vortex. This effect can be represented in the Kosterlitz-Thouless scenario by ascribing a larger fugacity to hybrid vortices (where both l and r wind) than to single vortices.

The reduction of symmetry in real crystals leads to terms that couple the phase of l and r fields. Breaking the symmetry to D_{2d} means there are two orthogonal preferred directions of polarization; since these orthogonal directions are equivalent, this does not produce splitting in the quadratic terms, but as discussed in Ref. 11, there is splitting due to interactions that may be written as $|\psi_x|^4+|\psi_y|^4$; using Eq. (1) this is proportional to

$$|l+r|^4+|l-r|^4=2(|l|^2+|r|^2)^2+4(l^*r+lr^*)^2.$$

Breaking the symmetry yet further to C_{2v} means favoring a specific linear polarization, and this will introduce a splitting at quadratic order; such a term would take the form $(l^*re^{i\chi_0}+\text{H.c.})$. Both of the above terms can be written in the notation in Eq. (10) as a term

$$\delta H_p=\Delta_p\sum_i\cos[p(\theta_i^l-\theta_i^r)],$$

where $p=2$ describes the reduction to D_{2d} and $p=1$ the reduction to C_{2v}.

B. Effect of perturbations on phase diagram

The generalization of Eq. (10), including the perturbation δH_p, was first discussed by Granato *et al.*[25] They included hybrid vortices, but only with aligned phase windings. Their discussion is based on studying the renormalization group (RG) flow in the Coulomb gas formulation of the model, where the dynamic variables are the positions of vortices. Using their formalism it is straightforward to show that when $\Delta_p=0$, the effect of hybrid vortices is unimportant: while in principle hybrid vortices can generate long-range interactions between left and right vortices, this does not occur if the energies of aligned and antialigned hybrid vortices are equal, which is the case here.[29] This means that if $\Delta_p=0$ the transition is exactly the scenario assumed above, where a BKT transition occurs if either specie of single vortex proliferates.

As the hybrid vortices alone have no significant effect, the model is exactly that discussed by Granato *et al.*[25] Unfortunately perturbative RG cannot adequately describe the model with δH_p for $p\leq 4$; the RG calculation always tends to a phase in which some species of vortex or dual vortex proliferate, and perturbation theory breaks down.[26] In addition, since one possible scenario discussed below involves two

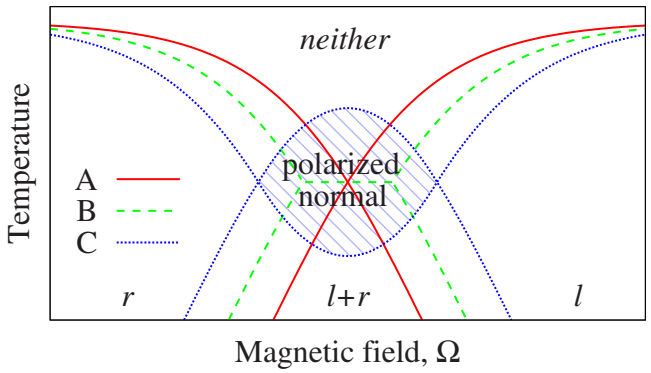

FIG. 3. (Color online) Possible topologies of phase boundary in the presence of $p=2$ (i.e., quantum well) symmetry breaking; A and B reflect Ref. 25, C contains the possible polarized but nonsuperfluid phase suggested by Ref. 27.

closely separated phase transitions, numerical approaches are challenging, as large system sizes are needed to prevent diverging correlation lengths near one phase boundary masking effects of the other.[27] For this reason, rather than a definite conclusion, the remainder of this paper discusses the various possible scenarios (Fig. 3) that have been proposed for δH_2, and their consequence for the polarized condensate. Granato *et al.*[25] suggest two possible topologies of the phase diagram: either the same as without δH_2 (option A), or with a region for $K^l \simeq K^r$ where there is a direct transition from the $f+g$ condensate to the uncondensed state (option B). Their suggestion was based on an argument[28] that when $K^l=K^r$ there can be only one transition. However, numerical simulations[27] of a closely related model[28] suggest that at $K^l=K^r$ there are two close but separate transitions: a higher temperature Ising transition where $\theta^l-\theta^r$ becomes locked at either 0 or π, and a lower temperature BKT transition where power-law correlations of average phase occur. For polaritons, this scenario (option C) implies an intermediate phase with linear polarization but no superfluidity. While polariton experiments might discriminate between these scenarios, this would be made difficult by the close spacing between the transitions, and the need for large homogeneous systems to avoid finite-size effects.

V. CONCLUSIONS

The phase diagram of polarized polariton condensate contains transitions between regions of circularly polarized condensates and elliptical polarizations. Comparing numerical and perturbative methods when the two polarizations decouple reveal limitations for the perturbative methods near the critical point, but they suggest that weak interactions between opposite polarizations have a small effect on the phase boundary. Terms which break the symmetry between different linear polarizations can change the topology of the phase diagram; such effects may however be very small, but present the possibility of using spinor condensates for experimental investigation of the topology of this phase boundary.

ACKNOWLEDGMENTS

I would like to thank N. R. Cooper, P. R. Eastham, and P. B. Littlewood for useful discussions, B. Svistunov for providing Ref. 17, Y. Rubo and A. Kavokin for comments on an earlier draft, and Pembroke College, Cambridge for financial support.

*jmjk2@cam.ac.uk

[1] J. Kasprzak *et al.*, Nature (London) **443**, 409 (2006).
[2] R. Balili, V. Hartwell, D. Snoke, L. Pfeiffer, and K. West, Science **316**, 1007 (2007).
[3] J. Kasprzak, R. André, L. S. Dang, I. A. Shelykh, A. V. Kavokin, Y. G. Rubo, K. V. Kavokin, and G. Malpuech, Phys. Rev. B **75**, 045326 (2007).
[4] F. M. Marchetti, M. H. Szymańska, J. M. J. Keeling, J. Kasprzak, R. André, P. B. Littlewood, and L. Si Dang, Phys. Rev. B **77**, 235313 (2008).
[5] A. P. D. Love *et al.*, Phys. Rev. Lett. **101**, 067404 (2008).
[6] K. G. Lagoudakis, M. Wouters, M. Richard, A. Baas, I. Carusotto, R. André, L. S. Dang, and B. Deveaud-Plédran, Nat. Phys. **4**, 706 (2008).
[7] S. Utsunomiya *et al.*, Nat. Phys. **4**, 700 (2008).
[8] A. Kavokin, J. Baumberg, G. Malpuech, and F. Laussy, *Microcavities* (Oxford University Press, Oxford, 2007).
[9] J. Keeling, F. M. Marchetti, M. H. Szymańska, and P. B. Littlewood, Semicond. Sci. Technol. **22**, R1 (2007).
[10] I. A. Shelykh, Y. G. Rubo, G. Malpuech, D. D. Solnyshkov, and A. Kavokin, Phys. Rev. Lett. **97**, 066402 (2006).
[11] Y. G. Rubo, A. V. Kavokin, and I. A. Shelykh, Phys. Lett. A **358**, 227 (2006).
[12] Y. G. Rubo, Phys. Rev. Lett. **99**, 106401 (2007).
[13] P. Renucci, T. Amand, X. Marie, P. Senellart, J. Bloch, B. Sermage, and K. V. Kavokin, Phys. Rev. B **72**, 075317 (2005).
[14] R. A. Battye, N. R. Cooper, and P. M. Sutcliffe, Phys. Rev. Lett. **88**, 080401 (2002).
[15] N. Prokof'ev and B. Svistunov, Phys. Rev. A **66**, 043608 (2002).
[16] Y. Kagan, V. A. Kashurnikov, A. V. Krasavin, N. V. Prokofev, and B. V. Svistunov, Phys. Rev. A **61**, 043608 (2000).
[17] B. Svistunov, Ph.D. thesis, Kurchatov Institute, 1990.
[18] E. L. Ivchenko and G. Pikus, *Superlattices and Other Heterostructures*, Solid-State Sciences No. 110, 2nd ed. (Springer, Berlin, 1997).
[19] I. L. Aleiner and E. L. Ivchenko, JETP Lett. **55**, 692 (1992).
[20] R. Winkler, *Spin-Orbit Coupling Effects in Two-Dimensional Electron and Hole Systems*, Springer Tracts in Modern Physics Vol. 191 (Springer, Berlin, 2003).
[21] G. Malpuech, M. M. Glazov, I. A. Shelykh, P. Bigenwald, and K. V. Kavokin, Appl. Phys. Lett. **88**, 111118 (2006).
[22] G. Panzarini, L. C. Andreani, A. Armitage, D. Baxter, M. S. Skolnick, V. N. Astratov, J. S. Roberts, A. V. Kavokin, M. R. Vladimirova, and M. A. Kaliteevski, Phys. Rev. B **59**, 5082 (1999).
[23] K. V. Kavokin, I. A. Shelykh, A. V. Kavokin, G. Malpuech, and

P. Bigenwald, Phys. Rev. Lett. **92**, 017401 (2004).
[24] Y. Rubo, Presented at ICSCE4, 2008 (unpublished), http://www.tcm.phy.cam.ac.uk/BIG/icsce4/talks/rubo.pdf
[25] E. Granato, J. M. Kosterlitz, and J. Poulter, Phys. Rev. B **33**, 4767 (1986).
[26] B. Nienhuis, in *Phase Transitions and Critical Phenomena*, edited by C. Domb and J. L. Lebowitz (Academic, London, 1987), Vol. 11, p. 1.
[27] M. Hasenbusch, A. Pelissetto, and E. Vicari, J. Stat. Mech.: Theory Exp. **2005**, 12002.
[28] M. Yosefin and E. Domany, Phys. Rev. B **32**, 1778 (1985).
[29] TE-TM splitting can however modify this; see Ref. 24.